Check for updates

Received: 27 June 2023 | Revised: 14 November 2023 | Accepted: 17 January 2024

DOI: 10.1111/cobi.14255

Conservation Biology

CONTRIBUTED PAPER

Disentangling the biotic and abiotic drivers of bird–building collisions in a tropical Asian city with ecological niche modeling

David J. X. Tan[1] | Nicholas A. Freymueller[1] | Kah Ming Teo[2] | William S. Symes[3] | Shawn K. Y. Lum[4] | Frank E. Rheindt[5]

[1]Department of Biology and Museum of Southwestern Biology, University of New Mexico, Albuquerque, New Mexico, USA

[2]National Parks Board, Singapore, Singapore

[3]Organization for Economic Co-operation and Development, Paris, France

[4]Asian School of the Environment, Nanyang Technological University, Singapore, Singapore

[5]Department of Biological Sciences, National University of Singapore, Singapore, Singapore

Correspondence
David J. X. Tan, Department of Biology and Museum of Southwestern Biology, University of New Mexico, 219 Yale Boulevard NE, Albuquerque, NM 87131, USA. Email: david.tanjx@gmail.com

Article impact statement: Maxent modeling shows that blue light and forest proximity predict bird–building collisions and identifies collision hotspots in Singapore.

Abstract

Bird collisions with buildings are responsible for a large number of bird deaths in cities around the world, yet they remain poorly studied outside North America. We conducted one of the first citywide fine-scale and landscape-scale analyses of bird–building collisions in Asia and used maximum entropy modeling (as commonly applied to species distribution modeling) in a novel way to assess the drivers of bird–building collisions in the tropical city-state of Singapore. We combined 7 years of community science observations with publicly available building and remote sensing data. Drivers of bird–building collisions varied among taxa. Some migratory taxa had a higher relative collision risk that was linked to areas with high building densities and high levels of nocturnal blue light pollution. Nonmigratory taxa had a higher collision risk in areas near forest cover. Projecting our results onto official long-term land-use plans, we predicted that future increases in bird–building collision risk stemmed from increases in blue light pollution and encroachment of buildings into forested areas and identified 6 potential collision hotspots linked to future developments. Our results suggest that bird–building collision mitigation measures need to account for the different drivers of collision for resident and migratory species and show that combining community science and ecological modeling can be a powerful approach for analyzing bird–building collision data.

KEYWORDS
bird strikes, community science, Maxent, urban ecology, urbanization, window collisions

INTRODUCTION

Bird collisions with buildings are prevalent across cities worldwide and represent a significant source of urban avian mortalities (Klem, 1989; Loss et al., 2015). In North America alone, it is estimated that from 365 to 988 million birds die from building collisions annually (Loss et al., 2014), second only to the number of cat-predation-related mortalities (Loss et al., 2013).

Despite the global nature of this phenomenon, significant geographical and methodological biases exist in the understanding of bird–building collisions. For one, most bird–building collision studies have focused on temperate North America, specifically on migratory Nearctic species (Basilio et al., 2020). Relatively few studies have focused on the tropics, especially the Paleotropics (Basilio et al., 2020; Tan et al., 2017). Furthermore, most studies of bird–building collisions have been based on systematic surveys conducted at very fine spatial scales (survey transects ranging from 1 to 21 buildings, usually on university campuses or in city centers) (Elmore et al., 2020; Hager et al., 2017). Although results of these studies broadly suggest collision rates are correlated with urban abiotic factors, such as the glass area on building façades (Borden et al., 2010; Cusa et al., 2015; Hager et al., 2008), building size (Elmore et al., 2020; Hager et al., 2017), nocturnal light pollution (Lao et al., 2020; Longcore & Rich, 2004; Winger et al., 2019), regional urbanization (Hager et al., 2017), and biotic factors, such as vegetation density (Cusa et al., 2015) and vegetation proximity (Barton et al., 2017; Gelb & Delacretaz, 2009; Rebolo-Ifrán et al., 2019), the limited scale at which these surveys have been conducted means they are unlikely to capture the full heterogeneity of city landscapes (including urban and peri-urban areas). Extending such fine-scale surveys to a citywide scale is often logistically infeasible. Conversely, data from alternative survey strategies based on opportunistic community or citizen

David J. X. Tan and Nicholas A. Freymueller contributed equally to this work.

© 2024 Society for Conservation Biology.

science approaches (Bayne et al., 2012; Rebolo-Ifrán et al., 2019) are often difficult to quantitatively analyze owing to the lack of true absence data. Consequently, how bird–building collision risk varies across geographical space at local, regional, and global scales remains poorly understood.

One useful analytical approach that has largely been overlooked in the context of bird–building collisions is maximum entropy modeling, specifically Maxent (Phillips et al., 2006), which compares values of environmental predictor variables at locations of verified records against values of the same variables at random points in the study area (where the taxon has not been observed, but could have accessed). Although Maxent is more often used for modeling the distributions of living organisms, it is conceptually equivalent to apply Maxent to modeling the distribution of bird–building mortalities because the risk of bird–building collisions can be similarly described as a stochastic Poisson phenomenon with a probability density dependent on environmental covariates that are inferred to have a causal relationship with mortality occurrences (Elith et al., 2010). The ability of Maxent to model species distributions based on presence-only occurrences makes this method particularly suitable for analyzing unstructured community science data as long as sampling bias is accounted for. Maximum entropy modeling and other species distribution modeling-adjacent techniques have already been applied to examine other causes of mortality in birds, including from vehicle traffic (Gomes et al., 2008), power lines, and wind turbines (Smeraldo et al., 2020), based on community science data.

The city-state of Singapore is particularly interesting in this regard because it has a well-documented incidence of bird–building collisions (Low et al., 2017; Tan et al., 2017), likely owing to its high level of urbanization and landscape heterogeneity (Gaw et al., 2019). Even so, little is known about the drivers of the spatial pattern of bird–building collisions in Singapore. Community science observations have identified resident and migratory bird species that may be particularly susceptible to building collision mortalities, for example, pink-necked green pigeon (*Treron vernans*) and blue-winged pitta (*Pitta moluccensis*), but it remains unclear whether the drivers of collisions in Singapore differ among species (Elmore et al., 2020; Tan et al., 2017).

We addressed the gaps and methodological challenges in our understanding of bird–building collisions by analyzing a multiyear community science data set of bird–building collisions from Singapore with a novel application of maximum entropy models. We projected the Maxent models onto future conditions based on future land-use plans and predicted how collision risks in Singapore may change over the next 10–15 years. In so doing, we sought to demonstrate how Maxent-based analyses can be a powerful tool for modeling bird–building collision risks and can be used to inform urban planning and conservation.

METHODS

Study area, design, and community science records

This study was conducted in the island nation of Singapore (1.1°–1.4°N and 103.6°–104.1°E; ~725 km^2) located in the Sundaland biodiversity hotspot and along the East Asian–Australasian Flyway (Figure 1). We documented bird–building collision records in Singapore from 2013 to 2020 with an established community science approach, in which members of the public were encouraged to report sightings of dead birds to a public hotline as well as via social media (Low et al., 2017). We identified all reported sightings to species based on photographic documentation or, where possible, collected specimens and georeferenced all bird mortality reports where possible based on GPS coordinates obtained from Google Maps. We assessed the likely cause of injury or death based on several lines of evidence as described in Tan et al. (2017). Specifically, birds found at the base of buildings with signs of facial injury or head trauma were classified as building collision victims. We documented other forms of mortality, and birds with an unidentifiable cause of death were listed as unknown (Tan et al., 2017). Based on the bird–building collision records collected, we collated a database of confirmed bird–building collision records for which locality data were available and classified each record based on the species' migratory status, excluding introduced species and species with indeterminate migratory status (Appendix S1).

Finally, we spatially thinned occurrences to a single record per taxon per 100 × 100-m pixel. Thinning records helps ameliorate the effects of uneven sampling and is a regular step in data processing for Maxent modeling (Aiello-Lammens et al., 2015). In the context of avian building collisions, although the density and frequency of collision records could be informative regarding the underlying drivers of bird–building collisions, we nonetheless applied spatial thinning to prevent a few extremely well-sampled pixels from dominating the pattern, given the uneven and incomplete sampling of community scientists. Additionally, this type of Maxent modeling (see "Model generation" below) can only accommodate presence or background locations. With increased sampling completeness, future work ought to be able to incorporate collision density information to disentangle collision drivers more robustly.

We modeled responses of specific avian taxa by pooling phylogenetically similar species into taxonomic bins to increase sample sizes and prepared subsets of the full collision data set for taxa with at least 10 confirmed collision records. These taxon bins included migratory taxa, such as pittas (genus *Pitta*), bitterns (genus *Ixobrychus*), *Ficedula* flycatchers (genus *Ficedula*), and the black-backed kingfisher (*Ceyx erithacus*), and nonmigratory taxa, such as green pigeons (genus *Treron*) and the Asian emerald dove (*Chalcophaps indica*). We also prepared a separate

15231739, 0, Downloaded from https://conbio.onlinelibrary.wiley.com/doi/10.1111/cobi.14255 by National University Of Singapo, Wiley Online Library on [17/03/2024]. See the Terms and Conditions (https://onlinelibrary.wiley.com/terms-and-conditions) on Wiley Online Library for rules of use; OA articles are governed by the applicable Creative Commons License

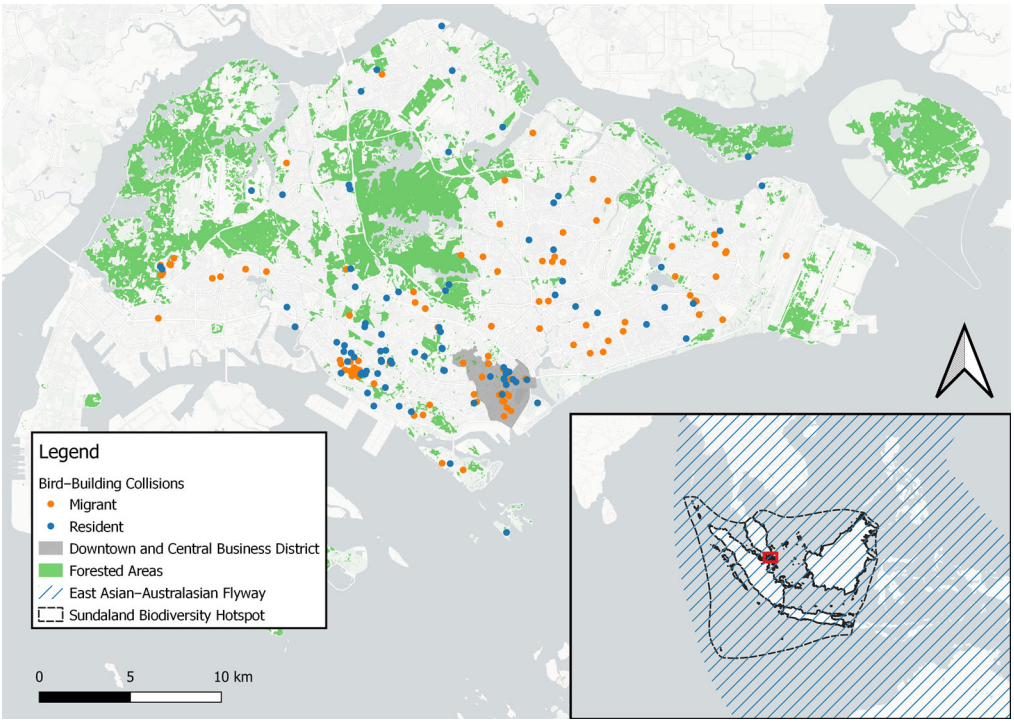

FIGURE 1 Map of bird–building collision localities in Singapore and Singapore's location relative to South and Southeast Asia, the Sundaland biodiversity hotspot, and the East Asian–Australasian Flyway (inset).

subset of collision records for all migrants and all residents (Table 1).

Abiotic environmental predictors

We built raster layers based on the spatial urban environment by downloading building polygons from the OpenStreetMap database (number of buildings 104,393) to model the effect of building size and density on bird–building collisions. OpenStreetMap contains a near-complete set of building polygons for Singapore (Biljecki, 2020) in shapefile format. We combined buildings with shared edges via the dissolve and multipart to singleparts functions in QGIS 3.14.16 because birds are unlikely to perceive subdivided buildings as separate entities. From the simplified building data set (number of buildings 72,448), we generated a 100 × 100-m rectangular pixel grid over the map extent and used the join attributes by location function in QGIS to extract building attribute summaries. To calculate per-pixel building perimeter, we used the polygons to lines function in QGIS to convert the building polygon data set into a series of lines and calculated the total line length contained in each 100 × 100-m pixel. We estimated mean building size per pixel by calculating the combined 2-dimensional floor area of all buildings intersecting each pixel divided by the number of buildings intersecting the pixel (details in Appendix S2). We estimated per-pixel building density by calculating the 2-dimensional area in the pixel covered by buildings for each pixel (Appendix S2). To generate a raster of building heights, we manually annotated building polygons from the full OpenStreetMap data set with building height data from Biljecki (2020) and OneMap 3.0 (https://www.onemap3d.gov.sg/main/, Singapore Land Authority), excluding sensitive structures such as government buildings and military installations. We subsequently coarsened the data set by applying a 100 × 100-m rectangular pixel grid over the map extent and used the join attribute by location function in QGIS to calculate per-pixel mean building heights.

We quantified effects of nighttime light pollution by downloading a true color night photograph of Singapore taken with a Nikon D4 with a 400-mm telephoto lens on 17 March 2016 by astronaut Tim Kopra from the International Space Station (NASA, 2016). We georeferenced the image in QGIS and decomposed the image into its red, blue, and green color channels. Because digital camera sensors convert incident light intensity into pixel values in the output image, the resultant red, blue, and green rasters reflect the intensity distribution of the respective light spectra across the nighttime urban landscape. We resampled all nighttime light pollution rasters with the r.resamp.interp() function in GRASS to a 100-m resolution with a bilinear interpolation.

Biotic environmental predictors

To generate rasters of vegetation density, we calculated the normalized difference vegetation index (NDVI) from a cloud-free multispectral image of Singapore captured by the LandSat8 OLI/TIRS platform (USGS). We applied the proximity (raster distance) function in QGIS to a rasterized map of Singapore's

15231739, 0, Downloaded from https://conbio.onlinelibrary.wiley.com/doi/10.1111/cobi.14255 by National University Of Singapo, Wiley Online Library on [17/03/2024]. See the Terms and Conditions (https://onlinelibrary.wiley.com/terms-and-conditions) on Wiley Online Library for rules of use; OA articles are governed by the applicable Creative Commons License

TABLE 1 Best-fit fine-scale (100 × 100 m) Maxent bird–building collision model loadings for each bird taxon and migratory phenology based on the Akaike's information criterion corrected for small sample sizes (AICc), variable percentage contribution, permutation importance (in parentheses), and model fit metrics.

Variable	*Pitta*	*Ficedula*	*Ixobrychus*	Migrants excluding *Pitta*, *Ficedula*, and *Ixobrychus*	All migrants	*Treron*	*Chalcophaps*	Residents excluding *Treron* and *Chalcophaps*	All residents
Mean building size	0	0.156 (0)	20.2 (11.2)	0.457 (0.539)	0.244 (1.18)	0	5.97 (8.48)	0	0.404 (2.88)
Building perimeter	2.51 (35.8)	6.57 (0)	3.21 (5.60)	0.224 (0.356)	4.90 (4.51)	0	0	0.0185 (0.227)	2.75 (6.84)
Building density	12.3 (13.27)	0	76.6 (83.2)	21.8 (20.3)	38.5 (36.0)	0	0	0	3.38 (6.48)
Mean building height	2.78 (16.8)	49.9 (25.4)	0	0.541 (1.42)	6.34 (5.92)	0	45.3 (28.0)	2.75 (5.96)	1.68 (6.49)
Blue light pollution	82.4 (34.1)	0	0	0.498 (3.18)	22.1 (6.21)	0	0	0	4.90 (3.26)
Red light pollution	0	0	0	2.91 (3.85)	1.50 (7.53)	0.307 (8.69)	0.00305 (0)	1.21 (0)	1.15 (1.87)
Normalized difference vegetation index (NDVI)	0	0	0	33.6 (19.6)	16.7 (21.8)	0	0.219 (1.14)	2.80 (4.48)	4.94 (9.27)
Forest proximity	0	43.4 (74.6)	0	39.9 (50.7)	9.86 (16.8)	99.7 (91.3)	48.5 (62.4)	93.2 (89.3)	80.8 (62.9)
Model fit metrics									
Feature classes	Q	LQP	LQP	LQP	LQP	Q	LQP	LQP	LQP
Regularization multiplier	5	2.5	1.5	3	5	4.5	2	4.5	4.5
Null AICc	695.517	328.5878	226.7771	1021.777	2265.757	715.907	308.2159	1062.562	2082.216
Model AICc	693.4262	326.0848	223.8886	1004.969	2257.009	702.6578	306.1208	1058.921	2053.675
Number of observations	35	16	11	50	114	35	15	52	105

15231739, 0, Downloaded from https://conbio.onlinelibrary.wiley.com/doi/10.1111/cobi.14255 by National University Of Singapo, Wiley Online Library on [17/03/2024]. See the Terms and Conditions (https://onlinelibrary.wiley.com/terms-and-conditions) on Wiley Online Library for rules of use; OA articles are governed by the applicable Creative Commons License

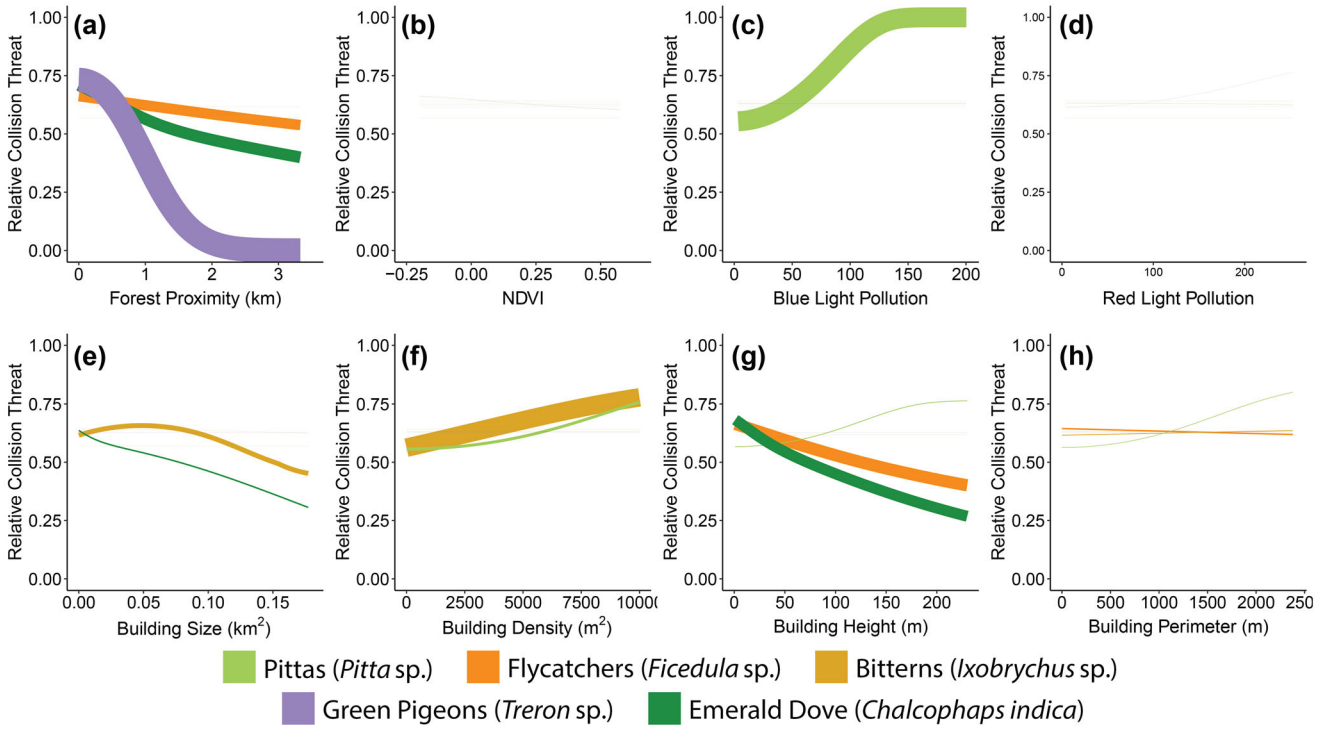

FIGURE 2 Avian taxon-specific collision risk response curves for 8 fine-scale ecogeographic variables: (a) forest proximity, (b) normalized difference vegetation index (NDVI), (c) nocturnal blue light pollution, (d) nocturnal red light pollution, (e) mean per-pixel building size, (f) total per-pixel building density (i.e., the area of a 100 × 100-m pixel occupied by buildings; an estimator of building density), (g) mean per-pixel building height, and (h) total per-pixel building perimeter (line thickness: relative contribution of the variable to the respective taxon-specific model).

forest cover in 2013 (Tan et al., 2018) to generate a forest proximity raster. These rasters were subsequently resampled to 100-m resolution with the GRASS GIS r.resamp.interp() function with a bilinear interpolation.

All predictor variable rasters and input shapefiles generated were reprojected to the SVY21/Singapore TM projection (EPSG:3414). A complete list of predictor variables is in Table 1 and Figure 2.

Calculating coarse-scale landscape effects

To investigate how collision risk varies with spatial scale, we generated coarsened versions of our predictor variable data set with the GRASS GIS r.neighbors() function, which resamples pixel values in a 500-m circular neighborhood. We generated coarsened focal rasters for all predictor variables except forest proximity, which allowed us to test the sensitivity of bird–building collisions at different spatial scales.

Creating future land-use change realization scenarios

To model how the distributions of bird–building collisions are expected to shift with land-use change, we generated a set of future land-use scenarios based on the 2019 Singapore Master Plan (Urban Redevelopment Authority, 2019), which maps out land-use strategies in Singapore for the next 10–15 years. We generated a simplified list of 11 land-use types based on the 2019 Master Plan (Appendix S3) and identified a subset of baseline polygons corresponding to areas where land-use change was not planned and a separate subset of polygons corresponding to areas earmarked for land-use change. We used QGIS to extract baseline values for each predictor variable and land-use type combination and the function fitdist() in the R package fitdistrplus (Delignette-Muller & Dutang, 2015) to fit a gamma distribution for each combination of land-use type and predictor variable with the maximum likelihood estimator method (Appendix S3). We used the gamma distribution because the predictor variables generally exhibit positive skewed distributions. With parameters obtained from the fitted gamma distributions, we used the create random raster layer (gamma distribution) function in QGIS to generate a random raster for each combination of predictor variable and land-use type (Appendix S3), clipped to the predicted land-use extent based on the 2019 Singapore Master Plan, for 5 independent replicates. For predictor variables with negative (e.g., NDVI) or very high pixel values (e.g., mean building size), we applied a transformation to the baseline raster values to facilitate gamma distribution fitting (Appendix S3) and subsequently corrected the transformation in the randomized predicted land-use rasters. We generated an overall land-use change raster for each independent replicate by using the r.series() function in GRASS GIS, which combines the predicted rasters for each land-use category into a single output raster and averages the pixel value

15231739, 0, Downloaded from https://conbio.onlinelibrary.wiley.com/doi/10.1111/cobi.14255 by National University Of Singapo, Wiley Online Library on [17/03/2024]. See the Terms and Conditions (https://onlinelibrary.wiley.com/terms-and-conditions) on Wiley Online Library for rules of use; OA articles are governed by the applicable Creative Commons License

for overlapping pixels with multiple land-use types. We used the raster calculator in QGIS to mask pixels in the original predictor variable rasters that intersect with the land-use change rasters and overlaid the land-use change rasters over the original predictor variable rasters.

Singapore is transitioning from high-pressure sodium vapor streetlamps (which emit red-orange light) to LED streetlights (which emit white light) (Land Transport Authority, 2017). We accounted for this transition by extracting present-day streetlight pollution values from the red-light pollution raster with a shapefile of Singapore's road network and adding varying proportions of present-day red-wavelength streetlight pixel values to the blue light pollution raster. This is based on the assumption that future LED streetlights will be maintained at a similar level of brightness as present-day sodium vapor streetlamps. We modeled 5 future blue light pollution scenarios ranging from 20% to 100% of present-day red light pollution levels (in increments of 20%) and generated 5 randomized future blue light pollution rasters per scenario based on the methods described above.

Predictor variable processing

To test for predictor variable collinearity, we used the r.covar() GRASS GIS function to calculate a covariance matrix for all possible pairwise comparisons of predictor variables and excluded the total building size, green light pollution, coarse-scale green light pollution, and coarse-scale mean building size predictors due to their high correlations with other predictor variables ($R > 0.8$) (Appendix S4). We masked predictor variable rasters to exclude areas where collision detection rates were likely to be anomalously low due to inaccessibility by community scientists, including military areas, nature reserves, high-security industrial zones, and airports (Appendix S5). Masking yielded a final tally of 26,821 random background points.

We used all available background points in our models because birds are highly dispersive and thus capable of occupying all available points. We avoided using a bias file to select background points because of the opportunistic nature of our community science data. Although a bias file could be used in Maxent to account for spatially uneven detection rates, there are multiple processes that positively and negatively influence whether community scientists detect bird carcasses. For example, high human foot traffic (e.g., in the Central Business District) and high reporting rates (e.g., on university campuses) could lead to a positive detection bias. However, high carcass removal rates by cleaners and pest control (Tan et al., 2017), especially in areas of high human traffic, and scavenging (e.g., by monitor lizards) are likely to decouple the relationship between observer density and positive detection bias. These spatially varying mechanisms are difficult to quantify robustly. Therefore, aside from spatial thinning to counter the effect of localized high reporting rates and masking areas with extremely low detection rates, we wanted to remain agnostic about how background points were weighted.

Model generation

We generated maximum entropy (Maxent v3.4.1; Phillips et al., 2017) models with a method based on the dismo 1.3-5 and kuenm 0.1.1 R packages (Cobos et al., 2019; Hijmans et al., 2015), as described in Freymueller (2020). We ran Maxent models with Q and LQP feature class combinations and regularization multiplier (β) values at 0.025, 0.05, 0.1, 0.25, 0.5, 0.75, and 1–5 (in breaks of 0.5) levels. To assess model fit, we used the small sample size-adjusted Akaike information criterion metric (AICc) (sensu Warren & Seifert, 2011) and selected models with the lowest AICc values ($\Delta AICc_{minimum} < 2$) and were markedly more likely than a null model ($\Delta AICc_{null}$ value >2). We applied this approach to ensure that our models were not unnecessarily complex or overfit, especially because some taxa had low sample sizes. After identifying the most likely models for each species, we visually inspected the response curves to ensure that they displayed ecologically plausible (i.e., not-concave-up) behavior. Per niche theory (Grinnell, 1917; Hutchinson, 1957), concave-up behavior of response curves is unlikely because if a species is found at both extremes of an environmental gradient, it should also be found at intermediate conditions. Models that displayed concave-up response curves were re-run after excluding problem variables from analysis. Whenever multiple models emerged with high support ($\Delta AICc_{minimum} < 2$), we compared them with 5-fold cross-validation and selected the model that had lower intramodel variability. We similarly performed cross-validation on models that emerged as the sole best-supported model to ensure they were not sensitive to slight changes in input data, which would suggest that they were overfit and not informative for model projection to new environmental conditions (Peterson & Samy, 2016). Following cross-validation, we generated weighted averages of all 5-folds into an ensemble model for each species. Weights were determined by multiplying testing sensitivity (given a training threshold of lowest presence [sensu Pearson et al., 2006]) by the partial area under the receiver operating characteristic curve (partialROC) at a defined omission of 0.01 across 500 iterations (Peterson et al., 2008). Testing sensitivity was appropriate to include as part of the model weights because it exists independent of any absence or fractional predicted area metric. We calculated partialROC metrics with the kuenm R package (Cobos et al., 2019); partialROC is more appropriate than traditional ROC-AUC-based metrics for correlative Maxent modeling given the lack of true absence data (Cobos et al., 2019; Peterson et al., 2008).

We ran Maxent models for 6 avian taxa (pittas (*Pitta* sp.), bitterns (*Ixobrychus* sp.), *Ficedula* flycatchers, black-backed kingfisher (*Ceyx erithaca*), green pigeons (*Treron* sp.), and Asian Emerald Dove [*Chalcophaps indica*]) and 4 additional models containing all migratory birds, all migratory birds excluding pittas, bitterns, and *Ficedula* flycatchers, all nonmigratory birds, and all nonmigratory birds excluding green pigeons and emerald doves (Table 1; Appendix S5). For all taxa, we ran one set of models with the fine-scale predictor variables (100-m resolution) and the other with the landscape-scale predictors (500-m resolution). We excluded Asian glossy starlings (*Aplonis panayensis*)

15231739, 0, Downloaded from https://conbio.onlinelibrary.wiley.com/doi/10.1111/cobi.14255 by National University Of Singapo, Wiley Online Library on [17/03/2024]. See the Terms and Conditions (https://onlinelibrary.wiley.com/terms-and-conditions) on Wiley Online Library for rules of use; OA articles are governed by the applicable Creative Commons License

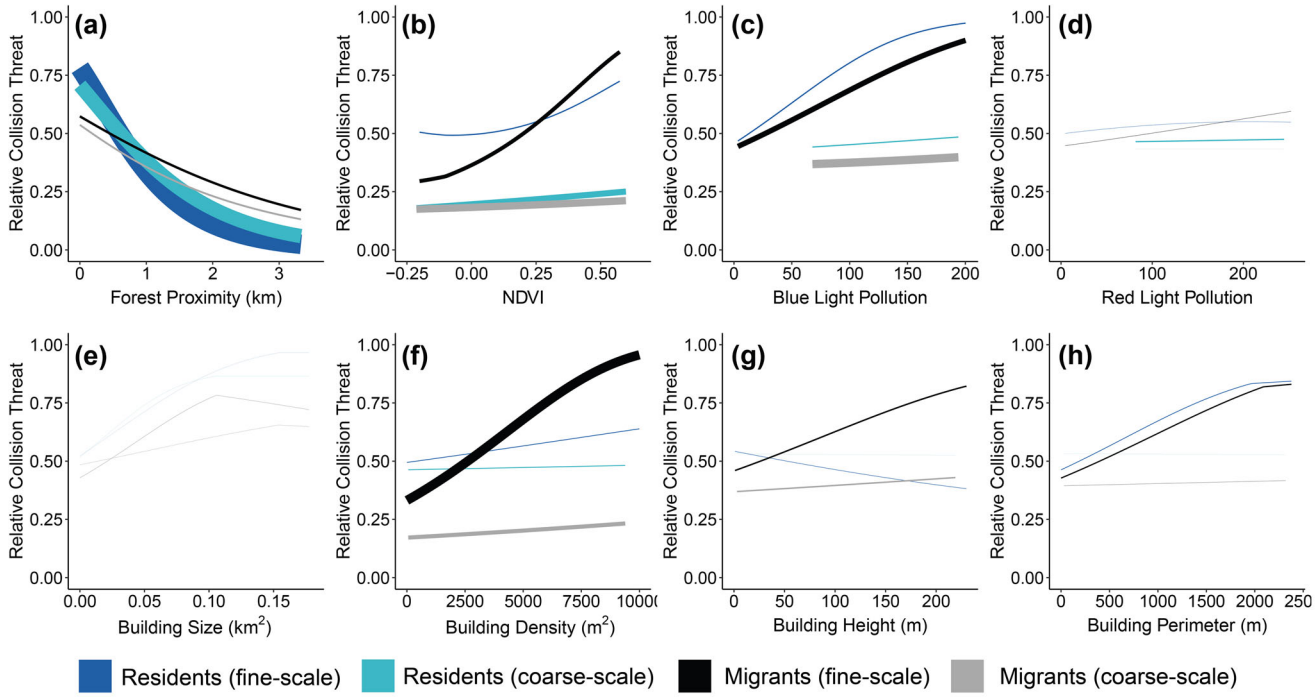

FIGURE 3 Relationship between relative collision risk and 8 ecogeographic variables for resident and migratory birds at different spatial scales (line thickness: relative contribution of the variable to the respective model).

from this analysis due to the relatively small number of occurrence records ($n = 6$) following spatial thinning. We projected the best models from the 100-m-resolution data set onto the full unmasked set of predictor variable rasters and plotted collision risk maps with the ggplot2 R package (Wickham, 2016) (Figure 3; Appendices S5A & S5C).

To assess if the patterns in our mortality models are not just driven by the distribution of living birds in Singapore, we downloaded modern occurrence records of living individuals from iNaturalist and eBird (Sullivan et al., 2009) on 14 October 2023 for 5 genera: *Chalcophaps*, *Ficedula*, *Ixobrychus*, *Pitta*, and *Treron*. We processed living records similarly to our collision records (including spatial thinning), constructed models in the same manner as our models on dead individuals, and compared suitability maps between these models and our models based on collision records. If collision drivers are nonrandom, the environments dead individuals are detected in should only be a partial subset of the environments living individuals are found in and should be more influenced by anthropogenic patterns (e.g., environments with less greenery, increased light pollution, and more buildings).

We generated future collision risk maps for each taxon by projecting the best model for each taxon onto all 5 predictor variable replicates for each of the 5 blue light pollution scenarios, for a total of 25 future collision risk maps. We generated a final forecast map for each taxon and blue light pollution scenario by averaging over the 5 replicates and plotted the maps with ggplot2 (Figures 5 & 6; Appendices S6 & S7). We ensured that these future projections were limited to areas with positive multivariate environmental similarity surface (MESS) (Elith et al., 2010) values to avoid making predictions in nonanalogous environmental space, where model transferability may be diminished (Appendices S9–S16). We calculated MESS values for each species model based on the final variables in that model, but all future projected scenarios ended up containing positive MESS values.

RESULTS

Bird–building collision records

We compiled a total of 224 confirmed bird–building collision records from 2013 to 2020 (mean of 34.3 detected collisions per year, range 12–51 observations annually), of which 114 were migrants and 105 were residents (Figure 1). Of the migrants recorded, 63.4% of collisions were composed of only 8 species (24% of total species richness), with 35 records (30.4%) for *Pitta* (*P. moluccensis* [27] and *P. sordida* [8]), 16 (13.9%) for *Ficedula* (*F. zanthopygia* [15] and *F. mugimaki* [1]), 11 (9.57%) for *Ixobrychus* (*I. flavicollis* [5], *I. cinnamomeus* [5], and *I. sinensis* [1]), and 11 (9.57%) for black-backed kingfisher. As for resident species, collision mortalities were dominated by pigeons (47.6%): 33 pink-necked green pigeon, 2 thick-billed green pigeon (*Treron curvirostra*), and 15 Asian emerald dove records.

Maxent model outputs

The variable coefficients and response curves of our Maxent models indicated that for each taxon group, collision risk was

15231739, 0, Downloaded from https://conbio.onlinelibrary.wiley.com/doi/10.1111/cobi.14255 by National University Of Singapo, Wiley Online Library on [17/03/2024]. See the Terms and Conditions (https://onlinelibrary.wiley.com/terms-and-conditions) on Wiley Online Library for rules of use; OA articles are governed by the applicable Creative Commons License

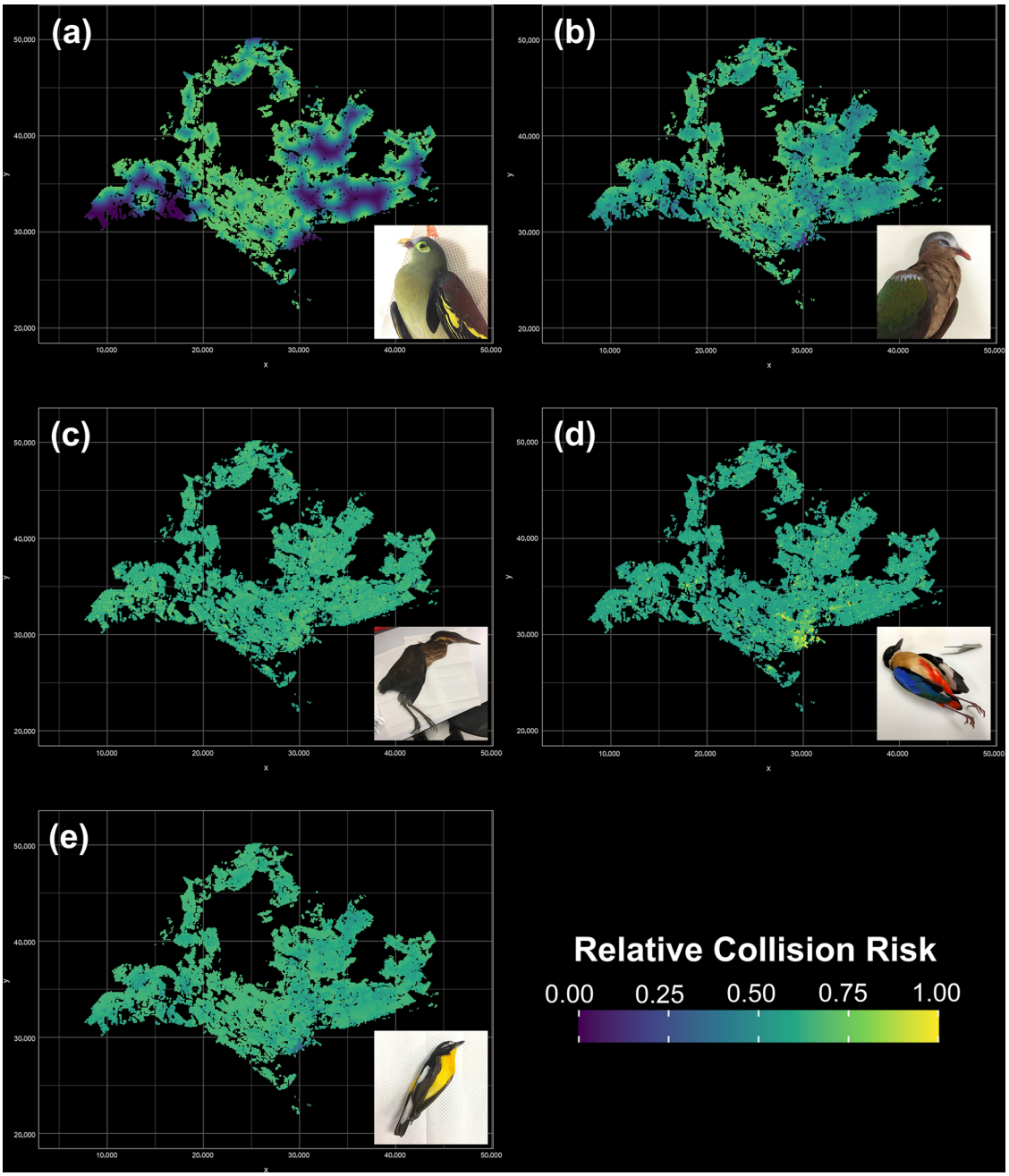

FIGURE 4 Bird–building collision risk maps for the 5 taxa that collide most frequently with buildings in Singapore based on fine-scale predictor variables: (a) green pigeons (*Treron* sp.), (b) Asian emerald dove (*Chalcophaps indica*), (c) bitterns (*Ixobrychus* sp.), (d) pittas (*Pitta* sp.), and (e) *Ficedula* flycatchers (*Ficedula* sp.). The collision risk values are relative (i.e., a collision risk of 1 does not equate to a 100% risk of collision).

explained by 2–3 high-contributing variables and that these high-contributing variables differed among taxa (Figure 2). In more general terms, our models suggested that forest proximity (Figures 2a & 3a) may be one of the most important predictors of bird–building collisions in the Southeast Asian tropics, affecting both resident and migratory taxa. In particular, our taxon-specific models suggested that low- to medium-rise buildings located near forest edge appeared to be collision hotspots for emerald doves and *Ficedula* flycatchers (Figure 4b,e). And, although building size and building perimeter (Figures 2e,h & 3e,h) did to some extent influence bird–building collision risk in bitterns and emerald doves, their effects were generally weaker relative to other predictor variables. Similarly, red light pollution (Figures 2d & 3d) appeared to have a considerably weaker effect on collision risk compared to blue light pollution. We did not observe any strong species-specific effect of vegetation density on collision risk and only observed a correlation between NDVI and collision risk in analyses broadly merging across multiple migratory species and, at landscape scales, nonmigrants (Figures 2b & 3b; Appendix S6).

15231739, 0, Downloaded from https://conbio.onlinelibrary.wiley.com/doi/10.1111/cobi.14255 by National University Of Singapo, Wiley Online Library on [17/03/2024]. See the Terms and Conditions (https://onlinelibrary.wiley.com/terms-and-conditions) on Wiley Online Library for rules of use; OA articles are governed by the applicable Creative Commons License

Across all migrants, the best-performing model indicated that building density was the strongest predictor of building collisions (38.5%), followed by blue light pollution (22.1%) and vegetation density (16.7%) at the fine scale (Table 1; Figure 3). The same variables were also identified in the landscape-scale model, although blue light pollution was the strongest predictor (34.8%), followed by vegetation density (30.3%) and building density (17.6%) (Appendix S6; Figure 3). For pittas in particular, high blue light pollution was the strongest predictor of collision at fine and landscape scales (82.4% and 78.2%, respectively) (Table 1; Appendix S6). For bitterns, high building density and building size were the main predictors of collisions, with fine-scale building density and building size explaining 76.6% (Figure 2f) and 20.2% (Figure 2e) of the best model, respectively (Table 1), whereas at landscape scales, the best model did not emerge as more likely than the null model (Appendix S6). Unlike for other migratory taxa, the best-performing model for *Ficedula* flycatcher collision risk encompassed forest proximity and low building height (43% and 49.9%, respectively) (Table 1). There was no clear pattern at coarser spatial scales (Appendix S6). We were unable to obtain any useful explanatory models for black-backed kingfishers, likely due to small sample size ($n = 11$). Excluding pittas, bitterns, and *Ficedula* flycatchers, collision risk for remaining migratory species was driven mainly by forest proximity (39.9% fine scale, 16.7% landscape scale), NDVI (33.6% fine scale, 44.0% landscape scale), and building density (21.8% fine scale, 18.7% landscape scale) at the fine and landscape scales (Table 1; Appendix S6).

Across resident species, the best-performing model at the fine scale identified forest proximity as the strongest predictor of bird–building collisions (80.8%); all other predictors had <10% contribution (Figure 3). At the landscape scale, forest proximity equally emerged as the best predictor of collision risk (59.5%) across resident birds, although NDVI also appeared to be a strong predictor (25.6%) (Figure 3). Both the best-performing fine- and landscape-scale models for *Treron* green pigeons identified forest proximity as the strongest predictor of building collisions (99.7% and 96.5% variable contribution, respectively) (Table 1; Appendix S6). Similarly, Asian emerald dove collisions were strongly linked to forest proximity at the fine and landscape scales (48.5% and 51.5% variable contribution, respectively) (Table 1; Appendix S6). The fine-scale model also identified low building height as a predictor (45.3%), and the landscape-scale model identified building density (43.9%) as a predictor. Excluding the green pigeons and emerald doves, collision models for the remaining resident species identified forest proximity as the strongest predictor at the fine and landscape scales (96.6% and 43.6%, respectively), whereas NDVI was also identified as a strong predictor in the landscape-scale model (29.1%). The second-best fine-scale model (ΔAICc = 0.234) and the best-fit landscape-scale models both identified blue light pollution as a weak but not insignificant collision predictor (22.1% and 10.3%, respectively), which suggests that blue light pollution may also be associated with collisions in some resident species as well.

Plotting the predicted collision distribution rasters for each taxon highlighted striking differences in the expected collision landscapes (Figure 4). Although the overall landscape-wide collision risk was high across all modeled taxa, for pittas and bitterns, collision hotspots appeared concentrated around the Central Business District and Downtown Commercial District, where building density and blue light pollution levels are high (Figure 4c,d). However, the bitterns also show elevated collision risk in industrial areas in the West. In contrast, the *Ficedula* flycatchers, pink-necked green pigeon, and Asian emerald dove were more likely to collide with buildings in areas close to forest cover, such as in areas fringing the central and southern forests (Figure 4a,b,e).

Comparison with living birds

Our living and dead bird models showed some similarities, but projections from models based on building-collision records were more associated with urban environments than projections from models based on living birds (Appendices S10–S14). This demonstrated that our bird–building collisions were not just a random sample of living bird distributions in Singapore. Collisions occurred in more built-up areas with lower NDVI values and higher light pollution (especially blue spectra) and that were farther away from forests relative to observations of live birds. Pittas exhibited the highest similarity between living and dead models (Appendix S13), but there was a strong difference in the areas of highest occurrence likelihood between the living and dead models for pittas, suggesting that the pitta mortality drivers are likely to differ from the drivers of live pitta occurrence.

Future collision landscapes

We found that future urban developments were likely to pose additional collision risks to birds strongly affected by forest proximity, owing to the encroachment of these developments into the edges of forested areas (Figure 5). In particular, new large-scale residential developments (zones 1–4 in Figure 5; Appendix S8) were predicted to be high-collision-risk zones for green pigeons, emerald doves, and *Ficedula* flycatchers due to their proximity to the central, western, and southern forest fragments. The incorporation of forest into new residential developments was predicted to contribute to higher collision rates as well. Our forecast models also showed that the proposed industrial development in Pasir Ris (zone 6 in Figure 5) is likely to be a collision risk zone for bitterns due to the projected high building density of this area. More importantly, an increase in blue light pollution was predicted to dramatically increase the landscape-wide collision risk for pittas, which constitute the largest proportion of collision records in the data set. Specifically, scenarios with blue light pollution levels exceeding 40% of present-day streetlight intensity were projected to increase the mean landscape-wide collision risk for pittas by at least 10.1% (Figure 6; Appendix S16).

As for the suitability of our model projections, our MESS analyses resulted in positive values, indicating our projections did not require extrapolation beyond the parameter limits of the

15231739, 0, Downloaded from https://conbio.onlinelibrary.wiley.com/doi/10.1111/cobi.14255 by National University Of Singapo, Wiley Online Library on [17/03/2024]. See the Terms and Conditions (https://onlinelibrary.wiley.com/terms-and-conditions) on Wiley Online Library for rules of use; OA articles are governed by the applicable Creative Commons License

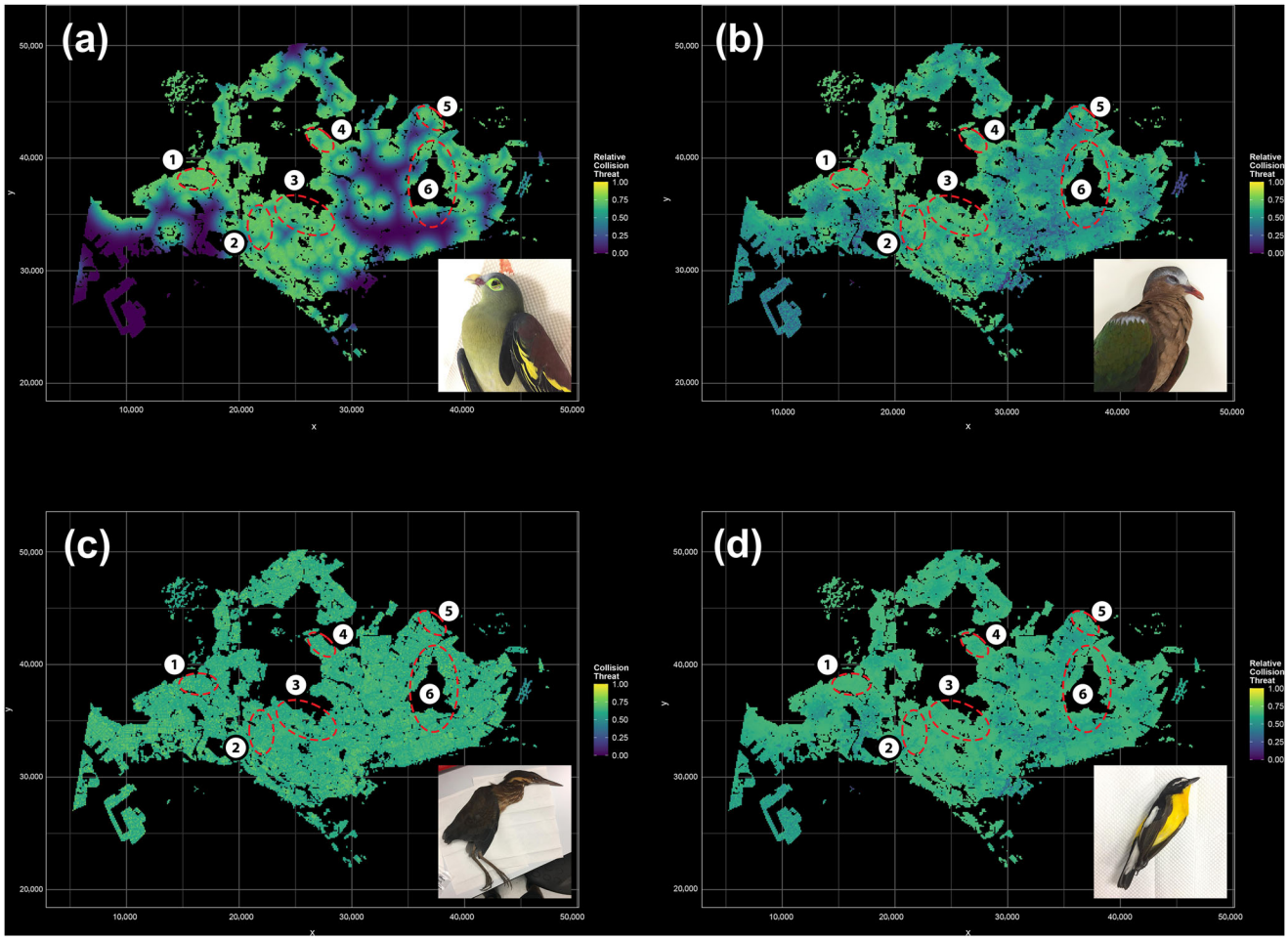

FIGURE 5 Projected future fine-scale bird–building collision risk maps for (a) green pigeons (*Treron* sp.), (b) Asian emerald dove (*Chalcophaps indica*), (c) bitterns (*Ixobrychus* sp.), and (d) *Ficedula* flycatchers (*Ficedula* sp.) based on the Singapore Master Plan 2019 (numbers, planning zones; zone 6, industrial). See Appendix S8 for a detailed breakdown of projected future developments.

training data set (Appendices S17–S24). However, some areas, such as the Central Business District, contained relatively lower MESS values in model projections, especially for models that incorporated blue light pollution as a predictor variable. This is because the Central Business District already contained relatively high levels of blue light pollution. The relative effect of these deviations likely did not affect our projections because the Central Business District was small relative to the overall projected area.

DISCUSSION

Suitability of maxent for modeling bird–building collisions

In addition to being the first multivariate analysis of bird–building collisions from Asia, our study is also one of the first to model the drivers of bird–building collisions at a landscape scale. Our results demonstrated that Maxent can produce robust model outputs with biologically meaningful inferences that provide baseline assessments of the collision risk landscape, all while leveraging opportunistically sampled community science data. Our ability to differentiate between the distributions of living and dead birds in Singapore at this spatial scale suggests our results were not a function of biases related to the underlying environmental data, which is a concern with this modeling approach (Warren et al., 2021). Collision risk maps, such as ours (Figures 4–6), can be used to prioritize high-collision-risk areas for targeted mitigation efforts. Furthermore, the ability to project models onto future development scenarios makes this tool potentially useful for urban planners and policymakers to facilitate the incorporation of preemptive collision mitigation measures into development plans.

Drivers of bird–building collisions

Similar to studies from North America (Elmore et al., 2020; Loss et al., 2019), we found that the main drivers of bird–building collisions varied among taxa. In contrast to those studies, however, building size was a relatively poor predictor of

15231739, 0, Downloaded from https://conbio.onlinelibrary.wiley.com/doi/10.1111/cobi.14255 by National University Of Singapo, Wiley Online Library on [17/03/2024]. See the Terms and Conditions (https://onlinelibrary.wiley.com/terms-and-conditions) on Wiley Online Library for rules of use; OA articles are governed by the applicable Creative Commons License

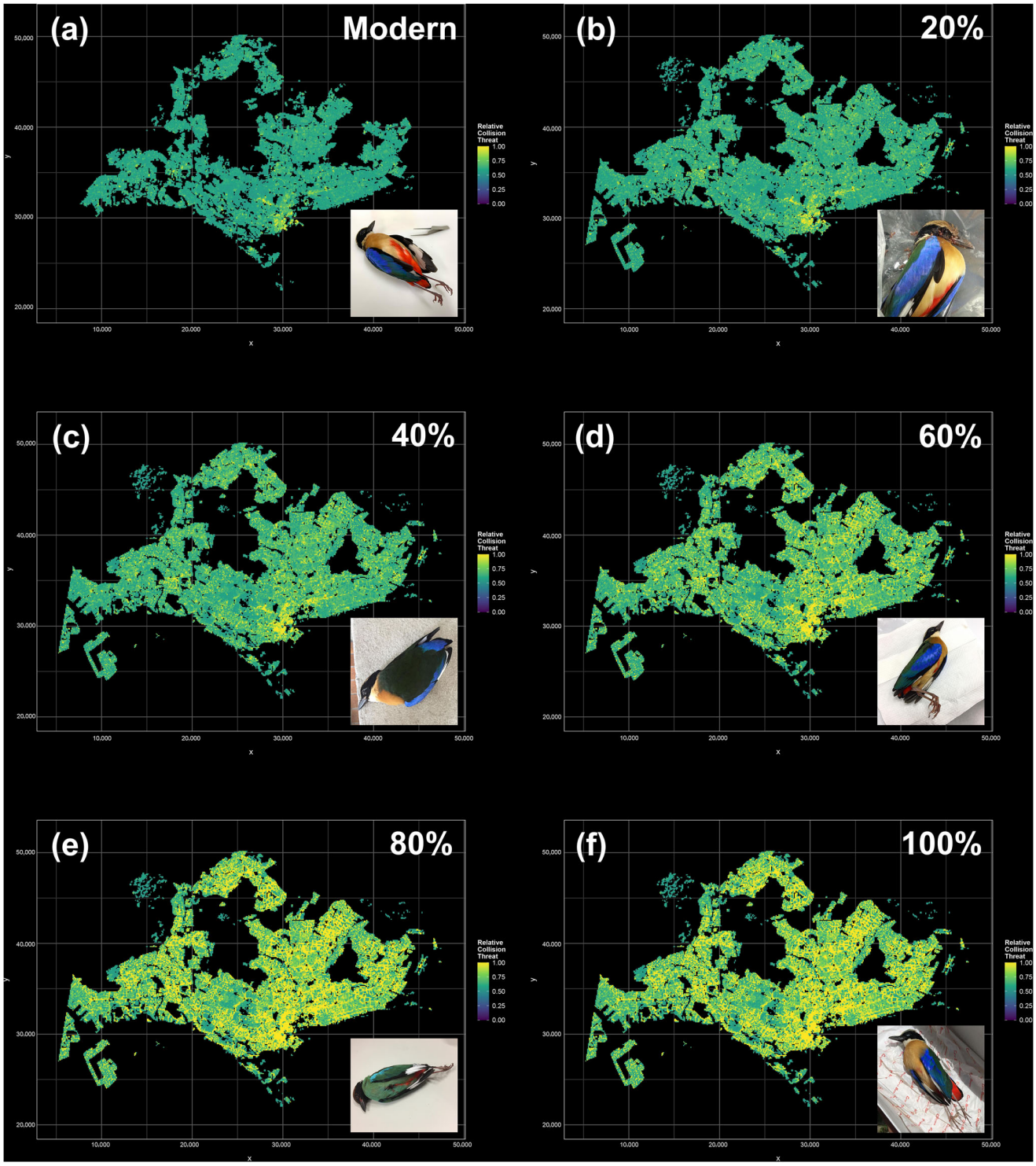

FIGURE 6 Forecast collision risk maps for the pittas (*Pitta* sp.) for 5 projected fine-scale scenarios of future nocturnal blue light pollution resulting from Singapore's transition to white LED streetlights from red-orange sodium vapor lamps. These scenarios correspond to (a) 0% (i.e., modern-day), (b) 20%, (c) 40%, (d) 60%, (e) 80%, and (f) 100% increases in blue light output relative to present-day levels of red streetlight pollution and suggest that a >40% increase in blue light pollution is likely to lead to major increases in landscape-wide relative collision risk.

15231739, 0, Downloaded from https://conbio.onlinelibrary.wiley.com/doi/10.1111/cobi.14255 by National University Of Singapo, Wiley Online Library on [17/03/2024]. See the Terms and Conditions (https://onlinelibrary.wiley.com/terms-and-conditions) on Wiley Online Library for rules of use; OA articles are governed by the applicable Creative Commons License

bird–building collisions; instead, building density (i.e., the overall space occupied by buildings per pixel), blue light pollution, forest proximity, and building height were better predictors of collision risk. It is unclear why building size emerged as a relatively good predictor in other studies, although it is possible that this may be a function of spatial scale. When contrasted against 100,000 buildings across an entire city, individual large buildings are less likely to be major obstacles to bird movement relative to dense clusters of buildings. Similarly, at very fine spatial scales, such as university campuses and city centers, where building densities are relatively high and homogeneous, the relative effect of individual large buildings should be comparatively stronger.

Increased blue light pollution and pitta collision risk

One of the more surprising results of this study was that blue light pollution was significantly associated with building collisions in pittas. Although the association between light pollution and increased collision risk is well-documented (Lao et al., 2020; Van Doren et al., 2021), relatively few studies have explored the impact of different light spectra (see Evans et al. [2007] and Poot et al. [2008] for exceptions). Although pittas are strongly attracted to bright lights during migration, as evidenced by historical records of high capture rates at One Fathom Bank lighthouse in the Straits of Malacca (Robinson & Boden Kloss, 1922) and at the spotlit MAPS banding station at Fraser's Hill, Malaysia (Wells, 1992), no specific attraction to blue light has been documented in this taxon to date. Our finding that blue, but not red, light pollution was associated with increased collision risk in at least one group of migratory birds in Singapore echoes a recent study by Zhao et al. (2020). They reported elevated catch rates of migratory birds at mist nets illuminated by blue light at night in Yunnan, China and suggested that future studies need to account for the differential effects of light color temperature on nocturnal migrants. However, our results also showed that this effect was not universal to all migratory species and suggested that migratory phototaxis toward particular light wavelengths may be a taxon-specific phenomenon. The strong effect of blue light pollution identified in the all-migrants model was likely driven solely by the abundance of pittas in the collision data set, and few other migratory birds in our data set exhibited strong attraction to light pollution at the scale of our analysis.

Regardless, our finding that pittas appeared acutely sensitive to blue light pollution is particularly concerning given recent changes to Singapore's light pollution profile. Although the bulk of blue light pollution in Singapore was restricted to downtown areas and shopping districts during our study period, since 2022 the Singapore government has replaced most of the country's sodium-vapor streetlights (which emit orange-red light) with LEDs (Abdullah, 2017), which has dramatically increased island-wide levels of blue light pollution. Our forecasting analyses indicated that increases in streetlamp-induced blue light pollution levels ≥40% of present-day red-light levels would likely to lead to significant increases in island-wide collision risk for migratory pittas (Figure 6).

A concerted effort by conservationists is thus needed to assess and reduce the potential impacts of the LED transition on migratory birds, not only in Singapore, but also in other cities located along migratory pathways. The LED transition underway in many developed countries is part of global efforts to reduce energy consumption and address climate change and is unlikely to be abandoned because of its impact on migrant birds. As such, solutions aimed at mitigating the negative effects of blue light on migratory birds could focus on attenuating the amount of blue light emitted by LED lights and other light sources during peak migratory months, such as by permanently or temporarily deploying LED streetlights with a lower color temperature (~2700–3000 K) that emit warmer, more red-shifted light, instead of LEDs that have a higher color temperature (~4000–5000 K) and emit cooler light with a higher blue fraction. Other solutions may be architectural or design related in nature, such as addressing the way light is directionally shielded, thereby minimizing the exposure of blue light to overflying birds. Further research is needed into the physiological effects of blue light on night-migrating birds and whether these effects are uniform across migratory avian taxa, especially because attraction to light pollution did not appear to be exhibited by any other migratory species in our data set.

Forest edges as collision hotspots

Although forest proximity had not been identified previously as a driver of bird–building collisions, it is likely that the importance of this predictor is partly explained by higher densities of forest-dwelling species near forest edges relative to elsewhere in the urban matrix (Brisque et al., 2017; Sabo et al., 2016), which is known to correlate with increased chances of building collisions (Hager et al., 2008). At the same time, collision rates are likely exacerbated by the fact that forest-dwelling frugivores, such as green pigeons and emerald doves, are highly dispersive and move between forest patches to forage (Cros et al., 2020), thereby encountering buildings near the forest edge. It is unclear, however, why other edge-dwelling frugivorous species, such as bulbuls or barbets, appeared to be less affected by bird–building collisions, especially because barbets are strongly overrepresented in building collision reports in other East Asian localities, such as Taiwan (Wang Ling-Min & Hsieh Chih-Heng, personal communication). Forest proximity also emerged as a driver of collision risk in some migratory taxa, such as yellow-rumped flycatchers, but not in others, such as pittas. Yellow-rumped flycatchers migrate during the night and seek out forest patches similar to their breeding habitat during the day to forage and rest on migration, putting them at greater risk of collision with buildings in forest-adjacent areas. Our finding that forest proximity is a strong predictor of collisions in migratory and nonmigratory taxa suggests that buildings near forest habitats are hotspots of bird collisions and are therefore sites most in need of collision mitigation measures.

15231739, 0, Downloaded from https://conbio.onlinelibrary.wiley.com/doi/10.1111/cobi.14255 by National University Of Singapo, Wiley Online Library on [17/03/2024]. See the Terms and Conditions (https://onlinelibrary.wiley.com/terms-and-conditions) on Wiley Online Library for rules of use; OA articles are governed by the applicable Creative Commons License

Addressing this issue is especially important in the context of Singapore due to the impending development of new residential and industrial estates adjacent to and in existing forested areas (Figure 5; Appendix 7). In particular, efforts by the Singapore government to retain forest patches in new residential developments, such as in the Tengah Forest Town (zone 1 in Appendix S8) (Tan et al., 2021) and Springleaf estate (zone 4 in Appendix S7) (Ng, 2022), with the intention of preserving biodiversity and forest connectivity could result in increased collision risks for resident and migratory birds. Modeling how future land-use change might affect bird–building collision risks will enable urban planners and architects to incorporate preemptive mitigation measures, such as bird-safe glass, louvers, and mullions, into building facades at the design phase, as is presently being explored in Springleaf estate (Ng, 2022), which would likely be more cost-effective than retrofitting buildings post hoc.

To a lesser extent, we also observed that vegetation density was broadly correlated with collision risk for migratory and nonmigratory species, especially at coarser spatial scales, although we did not observe any correlation between vegetation density and any of the species that collided most often with buildings. Although vegetation density may play a role in attracting migratory and nonmigratory birds at coarse scales, at finer spatial and taxonomic scales, vegetation quality likely matters more in determining the risk of building collisions. Alternatively, our results could also point to the limitations of the NDVI metric as a measure of vegetation density. Alternative metrics, such as the leaf area index (LAI) or enhanced vegetation index (EVI), should be considered in future work.

Our research highlights how the drivers of bird–building collisions may differ between temperate and tropical latitudes. The relative abundance of nonmigratory forest-dwelling frugivores, such as green pigeons and emerald doves, in tropical forests, combined with the elevated susceptibility of tropical pigeons to building collisions (Ocampo-Penuela et al., 2016; Santos et al., 2017), likely contributed to higher rates of nonmigratory bird–building collisions relative to temperate latitudes and thus the concomitant importance of forest proximity as a key driver of collision risk. More importantly, our results add to the long list of negative impacts of forest fragmentation, since fragmented forest landscapes are characterized by more edges with high collision frequencies.

Challenges and opportunities

Despite our data set spanning 7 years, large sample sizes were difficult to achieve because of the difficulty of diagnosing cause of death, relatively high carcass disposal rates across Singapore (Tan et al., 2017), and the highly heterogeneous detection rates of community scientists. Although Maxent may be a suitable method for analyzing opportunistically obtained bird–building collision data, some of our models performed poorly (e.g., black-backed kingfisher), likely pointing to the effect of small sample sizes. Combining community science with more systematic survey efforts may help address the sample size limitation as long as differences in survey effort are accounted for.

Our models benefited from the availability of highly detailed, fine- and landscape-scale open-source building data and land-use forecasts, which may be unavailable in many other countries. In the future, other predictor variables that are strongly associated with bird–building collisions, such as façade glass cover and amount of light reflected off glass façades, could be included in similar research (Hager et al., 2017; Lao et al., 2020). At present, these variables are challenging to quantify at the citywide scale. Future analyses should be able to address this limitation by combining emerging citywide 3-dimensional photogrammetric models with machine learning and computer vision methods to estimate fine-scale urban characteristics, such as glass area across entire cities.

Generating environmental predictor layers can also be challenging and time consuming. For example, generating the raster for building height in this study entailed manually annotating height data from individual buildings in the OneMap3D portal onto our shapefile of building polygons, which required approximately 2 months of continuous work to complete. With new computational methods, incorporation of such data should be more straightforward in the future.

The analytical approach we used can serve as a blueprint for more rigorous and applied analyses of bird–building collisions in cities worldwide. And, we hope that such analyses can subsequently be translated into policies aimed at reducing the incidence of bird–building collisions in urban areas.

ACKNOWLEDGMENTS

We thank the hundreds of community scientists from across Singapore who have contributed bird mortality records to this project. We also thank R. Chisholm, M. Foo, Y. Lin, and R. Meier for their support and assistance.

ORCID

David J. X. Tan https://orcid.org/0000-0001-7019-7871
Frank E. Rheindt https://orcid.org/0000-0001-8946-7085

REFERENCES

Abdullah, Z. (2017, January 4). LTA installing smarter, energy-saving street lights. The Straits Times. https://www.straitstimes.com/singapore/lta-installing-smarter-energy-saving-street-lights

Aiello-Lammens, M. E., Boria, R. A., Radosavljevic, A., Vilela, B., & Anderson, R. P. (2015). spThin: An R package for spatial thinning of species occurrence records for use in ecological niche models. *Ecography*, *38*(5), 541–545.

Barton, C. M., Riding, C. S., & Loss, S. R. (2017). Magnitude and correlates of bird collisions at glass bus shelters in an urban landscape. *PLoS ONE*, *12*(6), e0178667.

Basilio, L. G., Moreno, D. J., & Piratelli, A. J. (2020). Main causes of bird-window collisions: A review. *Anais da Academia Brasileira de Ciências*, *92*(1), e20180745.

Bayne, E. M., Scobie, C. A., & Rawson-Clark, M. (2012). Factors influencing the annual risk of bird–window collisions at residential structures in Alberta, Canada. *Wildlife Research*, *39*(7), 583–592.

Biljecki, F. (2020). Exploration of open data in Southeast Asia to generate 3D building models. *ISPRS Annals of Photogrammetry, Remote Sensing and Spatial Information Sciences*, *6*(2020), 37–44.

Borden, C. W., Lockhart, O. M., Jones, A. W., & Lyons, M. S. (2010). Seasonal, taxonomic, and local habitat components of bird-window collisions on an urban university campus in Cleveland, OH. *Ohio Journal of Science*, *110*, 44–52.

Brisque, T., Campos-Silva, L. A., & Piratelli, A. J. (2017). Relationship between bird-of-prey decals and bird-window collisions on a Brazilian university campus. *Zoologia*, *34*, 1–8.

15231739, 0, Downloaded from https://conbio.onlinelibrary.wiley.com/doi/10.1111/cobi.14255 by National University Of Singapo, Wiley Online Library on [17/03/2024]. See the Terms and Conditions (https://onlinelibrary.wiley.com/terms-and-conditions) on Wiley Online Library for rules of use; OA articles are governed by the applicable Creative Commons License

Cobos, M. E., Peterson, A. T., Barve, N., & Osorio-Olvera, L. (2019). kuenm: An R package for detailed development of ecological niche models using Maxent. *PeerJ*, *7*, e6281.

Cros, E., Ng, E. Y. X., Oh, R. R. Y., Tang, Q., Benedick, S., Edwards, D. P., Tomassi, S., Irestedt, M., Ericson, P. G. P., & Rheindt, F. E. (2020). Fine-scale barriers to connectivity across a fragmented South-East Asian landscape in six songbird species. *Evolutionary Applications*, *13*, 1026–1036.

Cusa, M., Jackson, D. A., & Mesure, M. (2015). Window collisions by migratory bird species: Urban geographical patterns and habitat associations. *Urban Ecosystems*, *18*, 1427–1446.

Delignette-Muller, M. L., & Dutang, C. (2015). fitdistrplus: An R package for fitting distributions. *Journal of Statistical Software*, *64*(4), 1–34.

Elith, J., Phillips, S. J., Hastie, T., Dudík, M., Chee, Y. E., & Yates, C. J. (2010). A statistical explanation of MaxEnt for ecologists. *Diversity and Distributions*, *17*, 43–57.

Elmore, J. A., Hager, S. B., Cosentino, B. J., O'Connell, T. J., Riding, C. S., Anderson, M. L., Bakermans, M. H., Boves, T. J., Brandes, D., Butler, E. M., Butler, M. W., Cagle, N. L., Calderón-Parra, R., Capparella, A. P., Chen, A., Cipollini, K., Conkey, A. A. T., Contreras, T. A., Cooper, R. I., … Loss, S. R. (2020). Correlates of bird collisions with buildings across three North American countries. *Conservation Biology*, *35*(2), 654–665.

Evans, W. R., Akashi, Y., Altman, N. S., & Manville, A. M. I. I. (2007). Response of night-migrating songbirds in cloud to colored and flashing light. *North American Birds*, *60*, 476–488.

Freymueller, N. F. (2020). *Niche dynamics of the felid guild following the Pleistocene Megafaunal Extinction* [Unpublished master's thesis]. University of New Mexico.

Gaw, L. Y. F., Yee, A. T. K., & Richards, D. R. (2019). A high-resolution map of Singapore's terrestrial ecosystems. *Data*, *4*, 116.

Gelb, Y., & Delacretaz, N. (2009). Windows and vegetation: Primary factors in Manhattan bird collisions. *Northeastern Naturalist*, *16*, 455–470.

Gomes, L., Grilo, C., & Mira, A. (2008). Identification methods and deterministic factors of owl roadkill hotspot locations in Mediterranean landscapes. *Ecological Research*, *24*, 355–370.

Grinnell, J. (1917). The niche-relationships of the California thrasher. *The Auk*, *34*(4), 427–433.

Hager, S. B., Cosentino, B. J., Aguilar-Gómez, M. A., Anderson, M. L., Bakermans, M., Boves, T. J., Brandes, D., Butler, M. W., Butler, E. M., Cagle, N. L., Calderón-Parra, R., Capparella, A. P., Chen, A., Cipollini, K., Conkey, A. A. T., Contreras, T. A., Cooper, R. I., Corbin, C. E., Curry, R. L., … Zuria, I. (2017). Continent-wide analysis of how urbanization affects bird-window collision mortality in North America. *Biological Conservation*, *212*, 209–215.

Hager, S. B., Trudell, H., McKay, K. J., Crandall, S. M., & Mayer, L. (2008). Bird density and mortality at windows. *The Wilson Journal of Ornithology*, *120*, 550–564.

Hijmans, R. J., Phillips, S., Leathwick, J., & Elith, J. (2015). *dismo: Species distribution modeling*. R package version 1.0-12. http://CRAN.R-project.org/package=dismo

Hutchinson, G. E. (1957). Concluding remarks. *Cold Spring Harbor Symposium on Quantitative Biology*, *22*, 415–427.

Klem, D. (1989). Bird-window collisions. *The Wilson Bulletin*, *101*, 606–620.

Land Transport Authority of Singapore. (2017). *Smarter and more energy-efficient street lighting system by 2022*. https://www.lta.gov.sg/content/ltagov/en/newsroom/2017/1/2/smarter-and-more-energy-efficient-street-lighting-system-by-2022.html

Lao, S., Robertson, B. A., Anderson, A. W., Blair, R. B., Eckles, J. W., Turner, R. J., & Loss, S. R. (2020). The influence of artificial light at night and polarized light on bird-building collisions. *Biological Conservation*, *241*, 108358.

Longcore, T., & Rich, C. (2004). Ecological light pollution. *Frontiers in Ecology and the Environment*, *2*, 191–198.

Loss, S. R., Will, T., Loss, S. S., & Marra, P. P. (2014). Bird–building collisions in the United States: Estimates of annual mortality and species vulnerability. *The Condor*, *116*, 8–23.

Loss, S. R., Will, T., & Marra, P. P. (2013). The impact of free-ranging domestic cats on wildlife of the United States. *Nature Communications*, *4*, 1396.

Loss, S. R., Will, T., & Marra, P. P. (2015). Direct mortality of birds from anthropogenic causes. *Annual Review of Ecology, Evolution, and Systematics*, *46*, 99–120.

Loss, S. R., Lao, S., Eckles, J. W., Anderson, A. W., Blair, R. B., & Turner, R. J. (2019). Factors influencing bird-building collisions in the downtown area of a major North American city. *PLOS ONE*, *14*(11), e0224164. https://doi.org/10.1371/journal.pone.0224164

Low, B. W., Yong, D. L., Tan, D. J. X., Owyong, A., & Chia, A. (2017). Migratory bird collisions with man-made structures in South-East Asia: A case study from Singapore. *BirdingASIA*, *27*, 107–111.

National Aeronautics and Space Administration. (2016). *Earth Observation image taken by Expedition 47 Crewmember*. https://www.flickr.com/photos/nasa2explore/25881524170/

Ng, K. G. (2022, June 6). Natural and built heritage to be conserved as Springleaf forested area is developed. The Straits Times. https://www.straitstimes.com/singapore/environment/natural-and-built-heritage-to-be-conserved-as-springleaf-forested-area-is-developed

Ocampo-Peñuela, N., Peñuela-Recio, L., & Ocampo-Durán, Á. (2016). Decals prevent bird-window collisions at residences: A successful case study from Colombia. *Ornitología Colombiana*, *15*, 84–91.

Ocampo-Peñuela, N., Winton, R. S., Wu, C. J., Zambello, E., Wittig, T. W., & Cagle, N. L. (2016). Patterns of bird-window collisions inform mitigation on a university campus. *PeerJ*, *4*, e1652.

Pearson, R. G., Raxworthy, C. J., Nakamura, M., & Townsend Peterson, A. (2006). Predicting species distributions from small numbers of occurrence records: A test case using cryptic geckos in Madagascar. *Journal of Biogeography*, *34*, 102–117.

Peterson, A. T., Papeş, M., & Soberón, J. (2008). Rethinking receiver operating characteristic analysis applications in ecological niche modeling. *Ecological Modeling*, *213*(1), 63–72.

Peterson, A. T., & Samy, A. M. (2016). Geographic potential of disease caused by Ebola and Marburg viruses in Africa. *Acta Tropica*, *162*, 114–124.

Phillips, S. J., Anderson, R. P., Dudik, M., Schapire, R. E., & Blair, M. E. (2017). Opening the black box: An open-source release of Maxent. *Ecography*, *40*(7), 887–893.

Phillips, S. J., Anderson, R. P., & Schapire, R. E. (2006). Maximum entropy modeling of species geographic distributions. *Ecological Modeling*, *190*, 231–259.

Poot, H., Ens, B. J., de Vries, H., Donners, M. A. H., Wernand, M. R., & Marquenie, J. M. (2008). Green light for nocturnally migrating birds. *Ecology and Society*, *13*(2), 47–60.

Rebolo-Ifrán, N., di Virgilio, A., & Lambertucci, S. A. (2019). Drivers of bird-window collisions in southern South America: A two-scale assessment applying citizen science. *Scientific Reports*, *9*, 18148.

Robinson, H. C., & Boden Kloss, C. (1922). Birds from the One Fathom Bank Lighthouse, Straits of Malacca. *Journal of the Federated Malay Straits Museum*, *10*, 253–255.

Sabo, A. M., Hagemeyer, N. D. G., Lahey, A. S., & Walters, E. L. (2016). Local avian density influences risk of mortality from window strikes. *PeerJ*, *4*, e2170.

Santos, L. P. S., de Abreu, V. F., & de Vasconcelos, M. F. (2017). Bird mortality due to collisions in glass panes on an Important Bird Area of southeastern Brazil. *Revista Brasileira de Ornitologia*, *25*, 90–101.

Smeraldo, S., Bosso, L., Fraissinet, M., Bordignon, L., Brunelli, M., Ancillotto, L., & Russo, D. (2020). Modeling risks posed by wind turbines and power lines to soaring birds: The black stork (*Ciconia nigra*) in Italy as a case study. *Biodiversity and Conservation*, *29*, 1959–1976.

Sullivan, B. L., Wood, C. L., Iliff, R. E., Bonney, D. F., & Kelling, S. (2009). eBird: A citizen-based bird observation network in the biological sciences. *Biological Conservation*, *142*, 2282–2292.

Tan, B. A., Gaw, L. Y. F., Masoudi, M., & Richards, D. R. (2021). Nature-based solutions for urban sustainability: An ecosystem services assessment of plans for Singapore's first "forest town". *Frontiers in Environmental Science*, *9*, 610155.

Tan, D. J. X., Yong, D. L., Low, B. W., Owyong, A., & Chia, A. (2017). Anthropogenic sources of non-migratory avian mortalities in Singapore. *International Journal of Tropical Veterinary and Biomedical Research*, *2*, 17–27.

Tan, D. J. X., Chattopadhyay, B., Garg, K. M., Cros, E., Ericson, P. G. P., Irestedt, M., & Rheindt, F. E. (2018). Novel genome and genome-wide SNPs reveal early fragmentation effects in an edge-tolerant songbird population across an urbanized tropical metropolis. *Scientific Reports*, *8*(1). https://doi.org/10.1038/s41598-018-31074-5

15231739, 0, Downloaded from https://conbio.onlinelibrary.wiley.com/doi/10.1111/cobi.14255 by National University Of Singapo, Wiley Online Library on [17/03/2024]. See the Terms and Conditions (https://onlinelibrary.wiley.com/terms-and-conditions) on Wiley Online Library for rules of use; OA articles are governed by the applicable Creative Commons License

Urban Redevelopment Authority. (2019). Singapore Master Plan 2019. Retrieved January 15, 2021, from https://www.ura.gov.sg/Corporate/Planning/Master-Plan

Van Doren, B. M., Willard, D. E., Hennen, M., Horton, K. G., Stuber, E. F., Sheldon, D., Sivakumar, A. H., Wang, J., Farnsworth, A., & Winger, B. M. (2021). Drivers of fatal bird collisions in an urban center. *Proceedings of the National Academy of Sciences of the United States of America*, *118*(24), e2101666118.

Warren, D. L., Dornburg, A., Zapfe, K., & Iglesias, T. L. (2021). The effects of climate change on Australia's only endemic Pokémon: Measuring bias in species distribution models. *Methods in Ecology and Evolution*, *12*, 985–995.

Warren, D. L., & Seifert, S. N. (2011). Ecological niche modeling in Maxent: The importance of model complexity and the performance of model selection criteria. *Ecological Applications*, *25*, 335–342.

Wells, D. R. (1992). Night migration at Fraser's Hill. *Bulletin of the Oriental Bird Club*, *16*, 21–25.

Wickham, H. (2016). *ggplot2: Elegant graphics for data analysis*. Springer-Verlag. https://ggplot2.tidyverse.org

Winger, B. M., Weeks, B. C., Farnsworth, A., Jones, A. W., Hennen, M., & Willard, D. E. (2019). Nocturnal flight-calling behaviour predicts vulnerability to artificial light in migratory birds. *Proceedings of the Royal Society B: Biological Sciences*, *286*, 20190364.

Zhao, X., Zhang, M., Che, X., & Zou, F. (2020). Blue light attracts nocturnally migrating birds. *The Condor*, *122*, duaa002.

SUPPORTING INFORMATION

Additional supporting information can be found online in the Supporting Information section at the end of this article.

How to cite this article: Tan, D. J. X., Freymueller, N. A., Teo, K. M., Symes, W. S., Lum, S. K. Y., & Rheindt, F. E. (2024). Disentangling the biotic and abiotic drivers of bird–building collisions in a tropical Asian city with ecological niche modeling. *Conservation Biology*, e14255. https://doi.org/10.1111/cobi.14255

15231739, 0, Downloaded from https://conbio.onlinelibrary.wiley.com/doi/10.1111/cobi.14255 by National University Of Singapo, Wiley Online Library on [17/03/2024]. See the Terms and Conditions (https://onlinelibrary.wiley.com/terms-and-conditions) on Wiley Online Library for rules of use; OA articles are governed by the applicable Creative Commons License